

SEISMIC ANALYSIS OF A BSR IN THE DOVE BASIN (SOUTH SCOTIA SEA)

A. Mocnik¹, D. Civile², A. Del Ben¹, R. Geletti²

¹ Dipartimento di Matematica e Geoscienze, University of Trieste, Italy

² OGS, Trieste, Italy

Introduction. In this paper we report the results from the seismic analysis of the part of the seismic profile IT95-167 that crosses a main part of the Falkland Plateau (Del Ben and Mallardi, 2004), the Dove Basin, located in the south Scotia Sea, with a N-S direction (Fig. 1). This analysis shows the presence of a high amplitude reflector that cuts the folded reflections related to the sedimentary infilling of the Dove Basin and mimics the shape of the seafloor. This Bottom Simulating Reflector (BSR) lays at about 750 ms. TWT below the seafloor, which is at a depth of more than 4200 m.

The Dove Basin is an oceanic basin bordered by the Pirie and Bruce Banks, respectively to its west and east margins, and by the continental slope of the South Scotia Ridge, to the south. It shows a roughly sigmoidal shape with an abyssal plain characterized by an average depth of about 3500 m. A prominent NNE-SSW elongated ridge (Dove Ridge), about 50 km long, is positioned in the central part of the basin and it is considered as an extinct spreading centre (Eagles *et al.*, 2005; Galindo-Zaldivar, 2014).

The seismic facies and the geometrical setting of the anomalous reflector identified suggested us to explore the origin of this BSR. Somoza *et al.* (2014) highlighted the presence of BSRs at three different levels in the Scan Basin located immediately to the east of the Bruce Bank. The authors interpreted the two deeper BSRs as fossil diagenetic fronts caused by elevated geothermal gradients respectively during the early and the middle Miocene; while the shallowest BSR would be originated by the presence of gas hydrates.

The presence of the seismic anomaly observed in the Dove Basin could be related to: 1) presence of Opal-A/Opal-CT transformation associated to a fossil diagenetic front; or 2) presence of a gas hydrate BSR in the Dove Basin. This second hypothesis should suggest the presence of abiogenic gas, derived by the serpentinization of basaltic rocks (Rajan *et al.*, 2012), which compose the oceanic basement of the Dove Basin.

- 1) Fossil diagenetic fronts are due to several varieties of silica minerals: amorphous quartz (opal-A), cryptocrystalline quartz (opal-CT/-C) and microcrystalline quartz (chalcedony, quartzine, etc). At low temperatures opal-A is generally precipitated inorganically or biogenically from natural aqueous solutions. During diagenesis siliceous deposits undergo mineralogical changes from opal-A to opal-CT/-C to microcrystalline quartz (Flörke *et al.*, 1982). This results in a density increase across the interface between the two forms of opal, producing a strong reflection with a positive polarity. This reflection follows

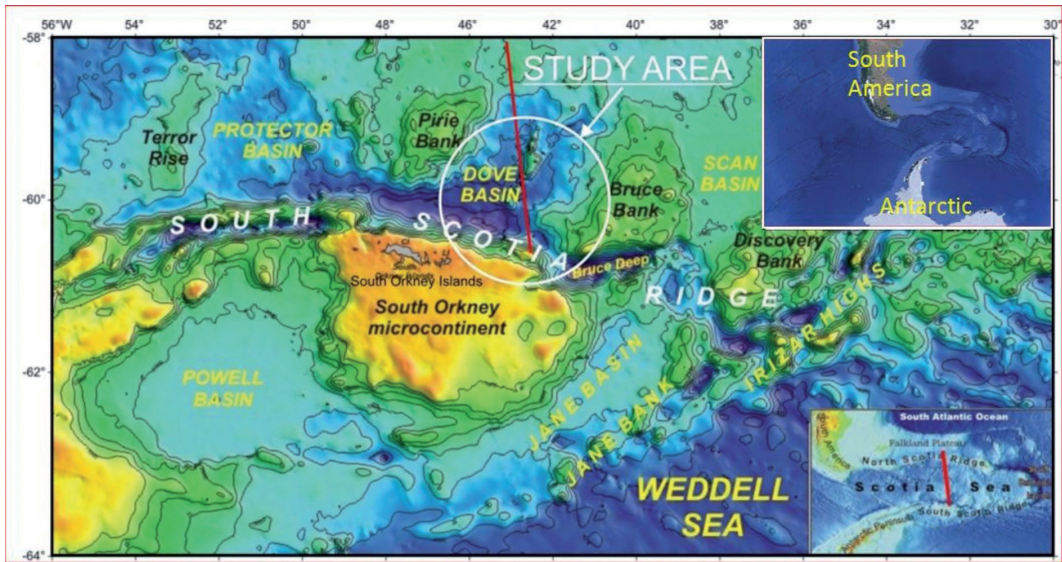


Fig. 1 – Physiographic map of the southern margin of the Scotia Sea, with the indication of the principal banks and basins. The study area is in the white circle.

an isothermal surface, mimicking and crosscutting the reflectors of the stratigraphic succession.

- 2) The gas-hydrate BSR displays high seismic amplitude with reverse polarity often accompanied by lowered frequency (low-frequency shadow) due to attenuation by free gas (Vanneste *et al.*, 2002). On a global scale, abiogenic or abiogenic CH_4 is produced in much smaller amounts respect biogenic CH_4 , and is generally not recognized in economically exploitable reservoirs. In many geological environments, biotic and abiogenic gases are mixed, and in many cases it is not easy to distinguish them. From scientific literature, magmatic process and gas-water-rock reactions trigger the production of abiogenic CH_4 (Etiope and Sherwood Lollar, 2013). The most widely abiogenic CH_4 generation mechanism in natural settings is the serpentinization of ultramafic rocks.

The two options presented are both compatible with the few available data on the geothermal gradient in the south Scotia Sea (yield values of 86.89 mW/m^2 at 2918 m water depth in the Scan Basin, Barker *et al.*, 2013).

During the year 2013, a sub-project has been presented and funded by the PNRA to explore these alternative possibilities in the context of the project VALFLU.

Geological setting. The Scotia Sea region is mainly of oceanic crustal structure and origin. It is bounded by the Drake Passage to the west and by the Scotia Arc on three sides. The Scotia Arc consists of the North and South Scotia Ridges, which are an assemblage of islands, submarine fragments of continental crust and deep basins, and of the South Sandwich island arc to the east. Oceanic magnetic anomalies suggest an Oligocene–Early Miocene age for the first sedimentary unit covering the basement of the Scotia Sea (MalDONADO *et al.*, 2006). Lindeque *et al.* (2013) highlighted a diachronic opening in the Scotia Sea (17.3–12.0 Myr): the oldest part would be near the Antarctic Peninsula, while toward northwest it becomes younger. The Dove Basin is a small NNE-SSW oriented sigmoidal depression located in the South Scotia Ridge. It is positioned between 60.5 and 58.5° S , and between 45 and 40° W , about 200 km long and 150 km wide. A NNE-SSW elongated ridge (Dove Ridge), about 50 km long, occupies the central part of the basin, where MORB-type tholeiitic basalt rocks have been recovered. In the basin depocenter, the sedimentary succession overlying the oceanic basement reaches more than 1.5-s TWT.

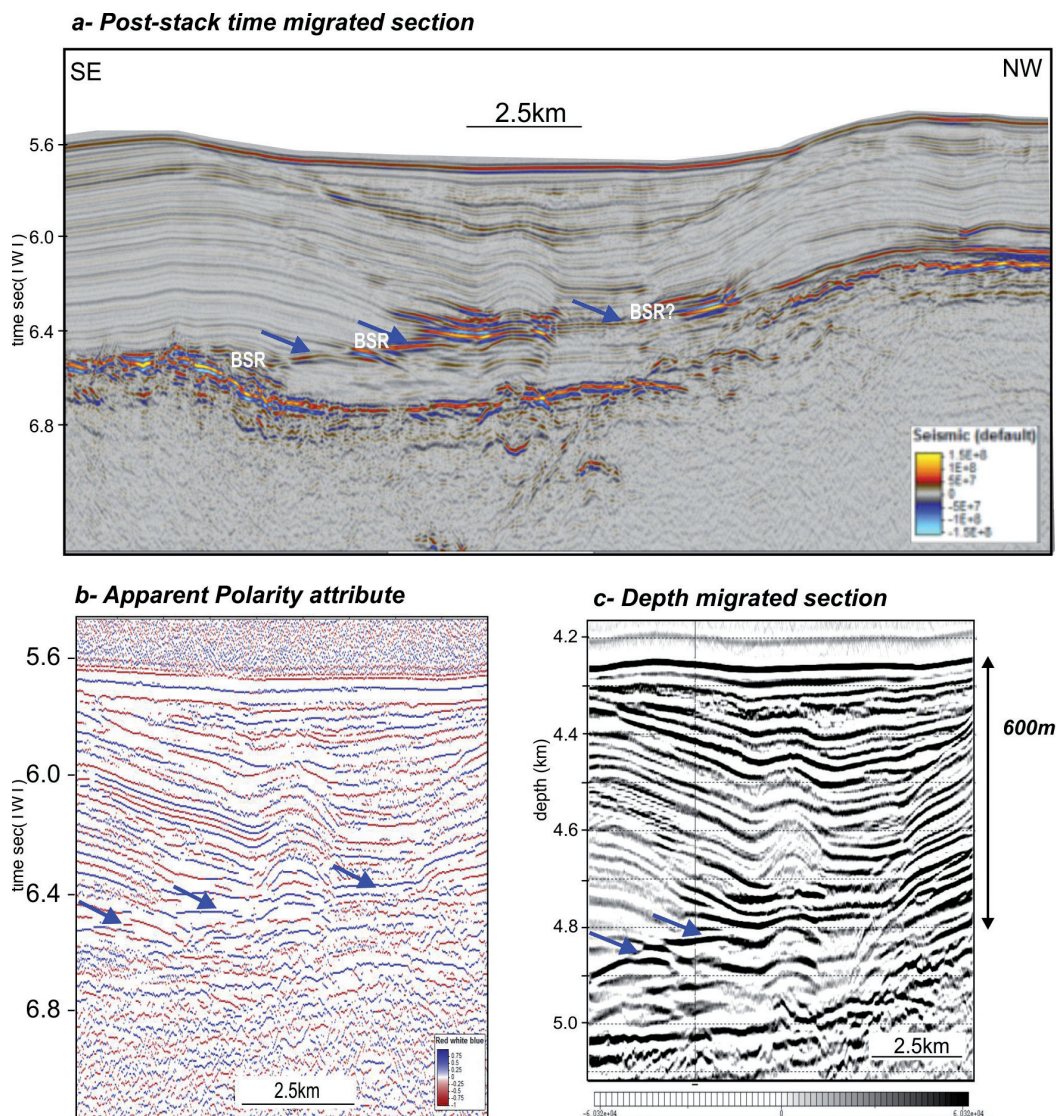


Fig. 2 – a) Portion of post-stack time migrated seismic profile I95-167 from SP1600 to SP2070; the blue arrows depict the extension of the observed BSR; b) application of Apparent Polarity seismic attribute obtained by Petrel software; the blue arrows indicate the position of BSR, which evidences a positive polarity; c) pre stack depth migrated section that let to reconstruct the real geometry of the layers and the depth of the BSR at about 600 m below the sea bottom.

Eagles *et al.* (2005) proposed an Eocene age (between 34.7 and 41 Myr) for the development of the Dove Basin, based on magnetic anomaly models and on the depth of the oceanic basement. Barker *et al.* (2013) suggested an age between 42 and 43 Myr for the oceanic crust, on the base of heat flow data. Galindo-Zaldivar *et al.* (2014) proposed, considering petrological, geochemical and geophysical data, integrated by absolute dating of dredge samples, that the Dove Basin was a back-arc basin developed from the Late Oligocene to the Early Miocene with a final volcanic episode at around 18 Myr.

Analysis of seismic data. *Seismic Data description.* The multichannel seismic reflection profile used in this work is the portion of the line IT95-167 crossing the Dove Basin in the south Scotia Sea. The data were collected by the Italian National Program for Antarctic Research

(PNRA) during the project SCOTIA (March 1995). The MCS data were acquired using an airgun source (combined chamber capacity of 80 l) and 120-channel seismic streamer with maximum offset of 3000 m. The recording parameters are: shot spacing 50 m, group interval spacing 25 m, CMP spacing 12.5 m and fold 30%. The total recording length is 15-s TWT and sample interval 4 ms; in this work, we considered the time window of 8-s TWT depth.

Along the analyzed seismic profile, the presence of a high amplitude reflector, which is almost parallel to the sea floor and cuts the reflections related to the sedimentary succession overlying the basement, is recognized at a depth of about 6.75-s TWT. It extends over about 600 CMP, covering a length of almost 7 km (Fig. 2a). These characteristics allow to define the recognized reflector as a BSR.

A BSR can be ascribed to:

- 1) a density increase across the interface between the two forms of opal, producing a strong reflection with a positive polarity;
- 2) the base of the stability zone (pressure and temperature conditions) of gas hydrates. Above a BSR, a solid phase of methane combined with water is present within a clastic matrix and this horizon produces an increment of the P-wave velocity. Below the BSR, free gas is present in the porous space of the rocks causing a drop of P-wave velocity. For this reason, the interface between the two gas phases is generally highlighted by a strong impedance contrast and high amplitude reflectors with negative polarity.

To analyze peculiar seismic features along the reflector, we re-processed the seismic profile focusing on the velocity analysis, depth migration and seismic attribute analysis.

Re-processing and pre-stack depth migration. We re-processed the portion of seismic profile using Focus (Paradigm) software, focusing on the velocity analysis of the acoustic wave across the interface; the first results of this analysis doesn't evidence clear velocity inversions along the entire length of the considered reflector.

A preliminary seismic attribute analysis of this reflector has been carried on to highlight the amplitude-phase and frequency characteristics.

The main objective of the use of attributes is to provide detailed information to the interpreter on structural, stratigraphic and lithological parameters of the seismic prospect. The attributes extraction allows to detect more easily some features that might not be directly observed on the original data and which are typically expressed by the attribute "amplitude". The benefit is to obtain the measured attributes at the same scale as the original seismic data.

A general definition of seismic attribute has been given by Chopra and Marfurt (2005). In the most general sense, they consider as seismic attributes all the quantities derived from a seismic data, including interval velocity, inversion of acoustic impedance, pore pressure prediction, reflectors termination and Amplitude Variation with Offset (AVO). This approach is useful in hydrocarbon exploration, because it contributes to improve the reservoir analysis and some attributes can be used as specific Direct Hydrocarbon Indicators.

Instantaneous amplitude, phase, cosine of phase and frequency attributes are the most effective to highlight the features of the observed BSR and could give a qualitative approach for a first ascription to one of the different hypothesis.

We analyzed the Apparent Polarity attribute to recognize possible phase inversion of acoustic wave at the base of BSR, due to solid/gas conversion below the Gas Hydrates Stability Zone (GHSZ). This attribute (Fig. 2b) shows in red-blue-red the phase behavior of the sea-bottom; the BSR shows the same passage of phase. Together with the velocity analysis, this represents a further result that reduces the possibility of a gas hydrate BSR.

Using Geodepth (Paradigm) software, we performed a further velocity analysis in order to convert root mean square values into interval velocity values using Dix equations. This led to create Common Depth Gather and to obtain a depth migrated sections (Fig. 2c).

This processing phase allowed to reconstruct the real geometry of the reflectors and to measure the thickness of the sedimentary sequence above the BSR. The water depth is at about

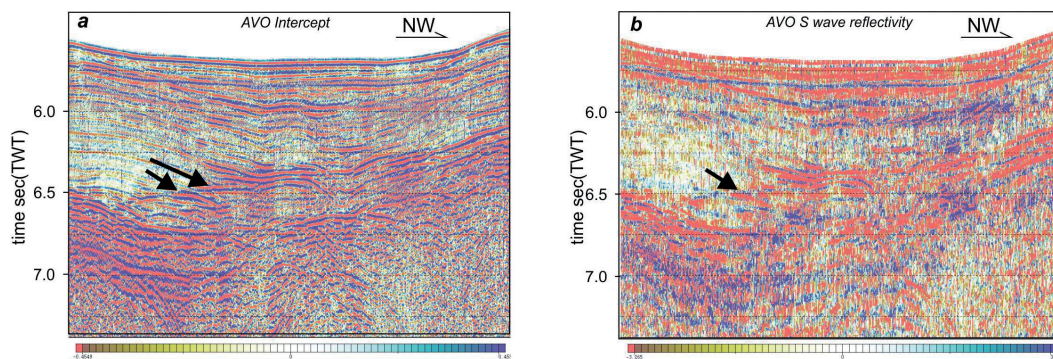


Fig. 3 – Application of AVO seismic attributes using Focus software (Paradigm) after true amplitude recovery by spherical divergence and generation of common angle gathers. In a), the result of AVO Intercept/P wave reflectivity at zero offset enhances the acoustic impedance in correspondence of the BSR, characterized by positive values; in b), the result of S wave reflectivity that shows a weak reflection in correspondence of the black arrow, denotes change of density across the interface.

4270 m and the thickness of sediments above the BSR ranges from 500-600 m. This value seems to be higher respect the common depth of the GHSZ.

AVO seismic attributes analysis. By the analysis of the P and S wave reflectivity, of the velocity values variation and of the components of the seismic data (amplitude, phase and frequency), we can obtain the information that allow to ascribe or not this seismic features to the presence of gas.

Nowadays, the AVO analysis has become a commercial tool for the oil industry; in particular, it lets geophysicists to better locate and classify gas or oil reservoirs, reducing the possibility of unproductive drills. The AVO techniques could be considered a good discriminator even in the case of gas-hydrate.

The offset-dependent reflectivity has its basis in the theoretical relationships between reflection coefficient, angle of incidence and variation of the compressional P wave velocity, shear S wave velocity and density across an interface; these contrasts are in turn dependent on rock properties variations. In presence of gas, brine-saturated and water-saturated unconsolidated sediments, these parameters have distinctive relationships; thus, using AVO analysis, bright spots caused by gas accumulation can be distinguished by mislead anomalous amplitude reflectors that could be caused by coal, cineritic or other low impedance units.

The AVO analysis is based on the observation and interpretation of the curves describing the variation of the Incident reflectivity with the angle of incidence (Castagna and Swan, 1997). Different AVO attributes have been extracted to apply multivariate analysis: the two most important are the zero offset reflectivity, defined Intercept, and the AVO Gradient, based on Shuey's approximation.

In presence of gas hydrates, the analysis of P- and S-wave reflectivity, which are related to the Poisson's ratio, gives important information on the fluid content and on rigidity of the solid matrix (Carcione and Tinivella, 2000). S-waves do not cross the fluid, so they are independent by the fluid contents showing changes of the solid matrix, which is due to the hydrocarbon hydrate compaction.

We analyze the P and S reflectivity by software Focus (Paradigm), which extract 9 AVO attribute sections from the generation of common angle gathers. For instance, the zero-offset extrapolated amplitude section is created on a sample-by-sample basis by transforming the data to the form of amplitude versus the trigonometric sin of the reflectance angle squared. A linear regression analysis is then performed and the fitted line is extrapolated to zero-offset, which forms the zero-offset section.

Similarly, the program creates a number of other sections, including a slope section (the slope of the fitted line), a product section (slope multiplied by the zero-offset amplitude), a Poisson's ratio section, and S-wave amplitude section. The latter two are formed from the zero-offset amplitude and the slope sections, using assumptions of small change in Poisson's ratio and an average V_p/V_s ratio of 2.0 (Poisson's ratio = 0.333).

For this analysis we prepared the original CDP by applying a band-pass filtering (cut frequencies 4-8/50-120 Hz) and in particular by the recovering the true amplitude of the reflected signal by spherical divergence correction.

Here we reproduce the results of the P-wave reflectivity and S-wave reflectivity in order to find their correlation. We observe (Fig. 3a) that across the BSR the P wave intercept is mainly characterized by positive values (blue color) and in particular by no relevant polarity inversion. On the other hand, the high amplitude reflection values could be significant of a change of fluids matrix properties of the material.

In Fig. 3b the S wave amplitude section has been obtained: it shows weak reflections in correspondence of the BSR. In association of what we observed on P wave reflectivity along the interface, even a change of density can be assumed.

Conclusions. The analysis of the portion of the seismic profile IT95-167 crossing the oceanic Dove Basin, located in the south Scotia Sea, has allowed to identify a high amplitude anomalous reflector that cuts the primary reflections assigned to the sedimentary infilling of the basin and mimic the shape of the seafloor. This type of signal could be interpreted as a BSR due to the gas hydrate layer or to an Opal-A/Opal-CT transformation zone.

Using different approaches to analyze this seismic BSR, we can synthesize our results as following:

- Velocity analysis: the velocity spectrum is ambiguous; a velocity inversion is not clear, but possible. Both the considered causes to explain the presence of the BSR could be realistic.
- Polarity attribute: not negative polarity has been highlighted by the polarity attribute analysis; this suggests an Opal -A/Opal-CT transformation.
- The measured thickness of the sediments above of the BSR seems to be higher than the common values of GHSZ; this turns away the hypothesis that the reflector could be related to gas hydrate.
- AVO: P and S-waves reflectivity only support density change across the BSR.

The comparison and integration of the different obtained results seem to be not sufficient to support the hypothesis of a gas hydrate BSR potentially associated to the presence of abiogenic gas in the sedimentary succession overlying the oceanic basement of the Dove Basin. On the contrary, an Opal-A/Opal-CT transformation seems to be a more plausible hypothesis. We intend to apply further analysis to better clarify the origin of the identified BSR.

Acknowledgements. The authors gratefully acknowledge Paradigm through the OGS Focus and Geodepth processing software, and Schlumberger through the University of Trieste Petrel academic grant for interpretation software.

References

- Barker P.F., Lawler L.A. and Larter R.D.; 2013: *Heat-flow determinations of basement age in small oceanic basins of the Southern central Scotia Sea*. Geological Society, London, Special Publications 381, 139-150.
- Carcione J. M. and Tinivella U.; 2000: *Bottom-simulating reflectors: seismic velocities and AVO effects*. Geophysics, **65**, 54-67.
- Castagna J.P. and Swan H.V.; 1997: *Principles of AVO crossplotting*. The Leading Edge, **16**, 337-342.
- Chopra S. and Marfurt K.J.; 2005: *Seismic Attributes-A historical perspective*. Geophysics, **70**(5), 3-28.
- Del Ben A. and Mallardi A.; 2004: *Interpretation and chronostratigraphic mapping of multichannel seismic reflection profile I95167, Eastern Falkland Plateau (South Atlantic)*. Marine Geology, **209**, 347-361.
- Eagles G., Livermore R.A., Fairhead J.D. and Morris P.; 2005: *Tectonic evolution of the West Scotia Sea*. Journal of Geophysical Research B: Solid Earth, **110**(2), 1-19.
- Etioppe G. and Sherwood Lollar, B.; 2013: *Abiotic Methane on Earth*. Reviews of Geophysics, **51**, 276-299.

- Flörke O. W., Köhler-Herbertz B., Langer K. and Tönges I.; 1982: *Water in Microcrystalline Quartz of Volcanic Origin: Agates*. Contrib. Mineral. Petrol., **80**, 324 - 333.
- Galindo-Zaldívar J., Puga E., Bohoyo F., Gonzales F.J., Maldonado A., Martos Y.M., Perez L.F., Ruano P., Schreider A.A., Somoza L., Surinach E. and de Fenerico Antonio D.; 2014: *Magmatism, structure and Age of Dove Basin (Antartica): A key to understanding South Scotia Arc development*. Global and Planetary Change, **122**, 50-69.
- Lindeque A., Martos Y.M., Gohl K. and Maldonado, A.; 2013: *Deep-sea pre-glacial to glacial sedimentation in the Weddell Sea and southern Scotia Sea from a cross-basin seismic transect*. Mar. Geol., **336**, 61–83.
- Maldonado A., Bohoyo F., Galindo-Zaldívar J., Hernández-Molina F.J., Jabaloy A., Lobo F. J., Rodríguez-Fernández J., Suriñach E. and Vázquez J.T.; 2006: *Ocean basins near the Scotia–Antarctic plate boundary: influence of tectonics and paleoceanography on the Cenozoic deposits*. Mar. Geophys. Res., **27 (2)**, 83–107.
- Rajan A., Mienert J., Bünz S. and Chand S.; 2012: *Potential serpentinization, degassing and gas hydrate formation at a (< 20Ma) young sedimented ocean crust of the Arctic Ocean Ridge system*. J. Geophys. Res., **117**, B03102, doi:10.1029/2011JB008537.
- Somoza L., Leon R., Medialdea T., Perez L.F., Gonzales F.J. and Maldonado A.; 2014: *Seafloor mounds, craters and depressions linked to seismic chimneys breaching fossilized diagenetic bottom simulating reflectors in the Central and Southern Scotia Sea, Antartica*. Global and Planetary Change, DOI: 10.1016/j.gloplacha.2014.08.004.
- Vanneste M., Guilard S. and Mienert J.; 2002: *Bottom-simulating reflections and geothermal gradients across the western Svalbard margin*. Terra Nova, **17**, 510-516.